conditions in technical applications and renders experimental measurements with these setups an excellent choice for investigating pollutant formation.
While predicting combustion phenomena and pollutants requires detailed models containing numerous species, considering all components of light volatiles and tars is neither feasible nor practical. Instead, the composition and properties of the actual fuel are often approximated by simplified surrogate formulations with a small number of representative components [57]. Besides various hydrocarbons, surrogate mixtures typically include oxygenated and nitrogen-containing species. Pyrolysis studies of algae, plant matter, and animal proteins identified the primary nitrogen-containing compounds in light volatiles and tar species [27, 64]. Among the light volatiles, ammonia (NH_3) and hydrogen cyanide (HCN) are the predominant nitrogen-containing species [23, 26, 55]. Chemical analyses of tars revealed pyrrole (C_4H_5N), pyridine (C_5H_5N), and piperazine ($C_4H_{10}N_2$) as the main nitrogen-containing compounds [3, 17, 19]. For oxygenated species, vanillin ($C_8H_8O_3$) and anisole (A_1OCH_3) were identified as key surrogate components [17, 19].
This chapter first evaluates the recent progress in modelling gas-phase chemistry for solid fuel combustion, focusing on oxyfuel conditions (Sec. 6.2). Several data sets of species mole fraction measurements obtained within the CRC/TR 129 ~~"Transregio 129"~~"Oxyflame" project and compiled from the literature are utilized to assess the progress in detailed kinetic modelling of PAHs and identify a detailed chemical kinetic model suitable for further investigations. The identified detailed model is amended by nitrogen chemistry and surrogate components relevant to biomass combustion, and subsequently reduced in a series of steps (Sec. 6.3). Concluding, we propose a compact kinetic model for the investigation of atmospheric, high-temperature combustion under oxyfuel conditions, which is suitable for simulating complex application cases at reduced computational costs.

6.2 Detailed modelling of PAH formation under oxyfuel conditions

Over the past decade, several studies advanced the understanding of gas-phase kinetics in biomass and coal combustion under oxyfuel conditions. Besides the C_0–C_4 core chemistry [4–6, 9, 14], the formation and oxidation of nitrogen-containing and oxygenated tars, such as pyrrole [15], pyridine [16], and anisole [13], were investigated through experimental, theoretical, and modelling work. These works demonstrated that the respective developed or analyzed models could describe the oxidation of small hydrocarbons and tars in reasonable agreement with experimental measurements under oxyfuel conditions. However, predicting pollutants, such as NO_x and PAHs, remains challenging [39], especially for oxygenated fuels [13, 30, 31], nitrogen-containing components [15], or complex mixtures of such species as they emerge from biomass devolatilisation [19].

upon the model of Cai et al. [10]. The most recent revision of the model by Hellmuth et al. [32] introduced updates to the C_7H_7 kinetics. This model [32] will be called the "ITV model" in the following. Besides an extensive revision of the PAH chemistry [32, 39, 40], Langer et al. [39, 40] introduced several updates to the C_0–C_4 core chemistry that are expected to impact combustion under oxyfuel conditions. For example, Langer et al. [39] updated the rate coefficient of the reaction $CO + OH = CO_2 + H$ based on the theoretical work of Senosiain et al. [59]. This reaction may be particularly significant under oxyfuel conditions because it sensitively influences hydrogen (H) radical availability [9], which may strongly affect PAH formation. Further modifications include the integration of the C_3 chemistry from the modelling work of Panigrahy et al. [50]. Baroncelli et al. [4] showed that C_3 chemistry plays a crucial role in aromatics formation from the non-premixed combustion of two of the most abundant devolatilisation products [4], methane and acetylene (C_2H_2). Updates to the PAH chemistry [39] that are expected to be particularly relevant include radical recombination reactions involving five-membered ring species. Reaction flux analysis of Chen et al. [13] for anisole counterflow diffusion flames suggests that introduced updates of the cyclopentadienyl radical self-recombination reactions ($C_5H_5 + C_5H_5$) are critical, as this was found to be the dominant naphthalene (A_2) formation pathway. The ITV model [32] is directly comparable to the model of Cai et al. [10] and was last updated in 2024. Hence, this is a another suitable reference point for evaluating recent progress in PAH modelling under oxyfuel conditions.

data

Figure 6.1 compares predictions obtained with the model of Cai et al. [10] and the ITV model [32] to ~~experimental~~ measurements for several fuels. The comparison considers data from time-of-flight mass spectrometry (ToF-MS) [4–6, 38, 48, 66] and gas chromatography (GC) [11, 21, 32], including investigations performed within the Transregio 129 Oxyflame project [4–6, 32], for cyclopentadiene (C_5H_6), benzene (A_1), phenylacetylene (A_1C_2H), styrene ($A_1C_2H_3$), ethylbenzene ($A_1C_2H_5$), indene (C_9H_8), naphthalene, and acenaphthylene ($C_{12}H_8$) when comparing the ITV model [32] to the model of Cai et al. [10]. The only exception is toluene (A_1CH_3), although the predictions remain accurate. The computed mean deviation factors [39] shown in the bottom right of the parity diagrams in Fig. 6.1 highlight a considerable improvement for phenylacetylene and acenaphthylene, whose mean deviation factors reduce by more than a factor of four. This quantitative evaluation illustrates that the ITV model [32] is suitable for investigating oxyfuel combustion and PAH formation. Therefore, it was chosen as the basis for developing a compact model for biomass combustion in the subsequent sections.

the sentence ends here
↳ rephrase!

6.3 Skeletal kinetic model for biomass surrogate components

Modelling the gas-phase chemistry of biomass fuels requires the description of the underlying chemistry that governs the volatilisation and gas-phase processes. However, a detailed representation of these processes results in complex chemical kinetic models, making their use computationally impractical in large-scale simulations. This section addresses the development of a skeletal, i.e., compact, chemical kinetic model suitable for large-scale simulations, which is based on the ITV model [32] discussed in Sec. 6.2. The skeletal model was specifically designed to predict the gas-phase chemistry of biomass fuels under conditions relevant to practical applications, including high-temperature atmospheric combustion in air or oxyfuel environments. Figure 6.2 illustrates the development process.

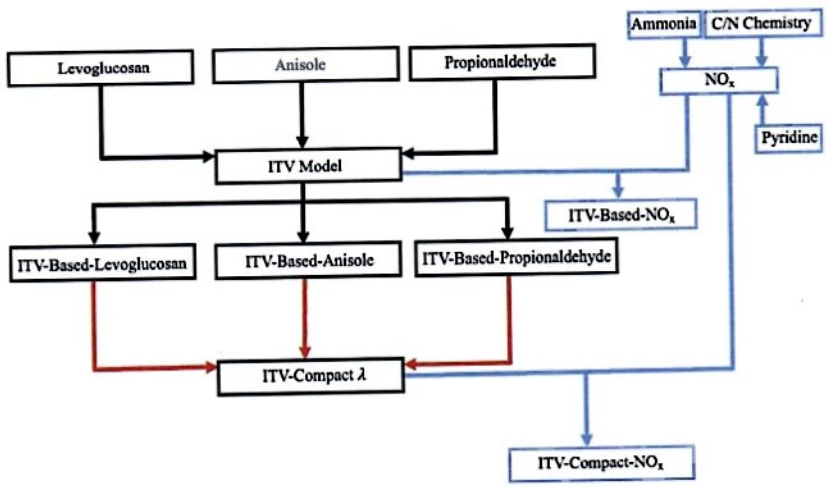

Fonts too small

Figure 6.2: Development process of the compact surrogate model. Black arrows denote the integration of tars surrogate components with the ITV model, red arrows indicate the reduction and merging steps, and blue arrows denote steps related to the development of the skeletal NO_x submodel and its integration with the other models.

Developing such a model first requires deriving a surrogate formulation to approximate the volatile mixture composition released from the fuels targeted in the numerical investigation. Here, the particle devolatilisation model proposed by Ranzi et al. [57] and further extended by Debiagi et al. [18] was applied to three different biomass particles: raw miscanthus, torrefied miscanthus, and torrefied corn straw. The particle devolatilisation model provides complex mixtures including light hydrocarbons, oxygenated species, aldehydes, tars, aromatics, and several nitrogen-containing species. The latter includes

was ensured among the core chemistry of the reduced models, and differences were primarily confined to the integrated tar-specific chemistry.
The validation of the ITV-Compact model considered zero- and one-dimensional configurations, including measurements of ignition delay times in shock tubes and species mole fractions in counterflow diffusion flames. Predictions from the ITV-Compact model were compared with those from the corresponding detailed model to quantify reduction effects. Furthermore, comparing the ITV-Based models to the reference models from which the chemistry of the integrated volatile species revealed the impact of different base chemistries. For a more extensive validation, the reader is referred to Farmand et al. [**Farmand2025submitted**].

Ignition delay times for small volatiles

Figures 6.3–6.5 show ~~experimental~~ measurements [28, 37, 43, 52] of ignition delay times for small volatiles under oxyfuel conditions in comparison with model predictions using the ITV-Compact and the ITV model [32]. Notably, the ignition delay times predicted with the ITV model [32] are in good agreement with the experimental data. The minor discrepancies between predictions obtained with ITV-Compact and the ITV model [32] indicate that the reduction process introduced no significant errors in the ignition delay time prediction.

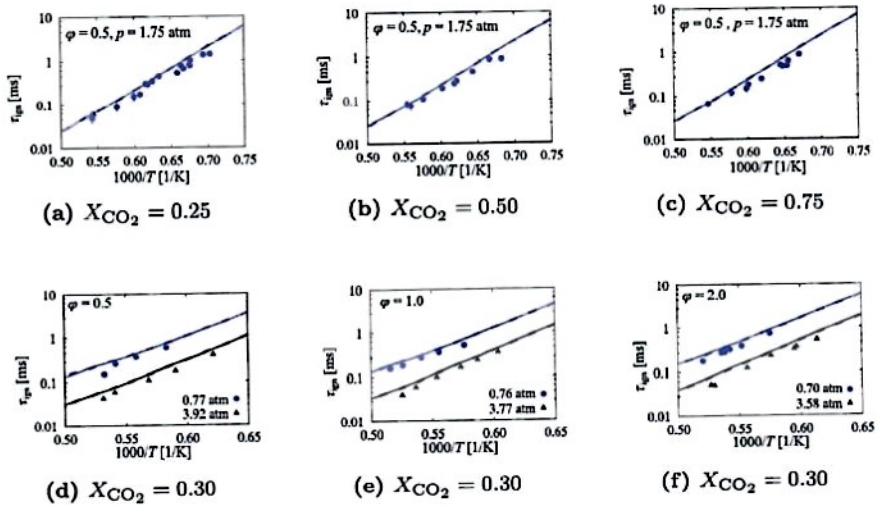

(a) $X_{CO_2} = 0.25$ (b) $X_{CO_2} = 0.50$ (c) $X_{CO_2} = 0.75$

(d) $X_{CO_2} = 0.30$ (e) $X_{CO_2} = 0.30$ (f) $X_{CO_2} = 0.30$

Figure 6.3: Comparison of ignition delay times of $CH_4/O_2/CO_2$/argon (Ar) mixtures at various pressures (p) and fuel-air equivalence ratios (φ) in a shock tube. Symbols denote the experimental data [28, 37], solid lines denote model predictions with the ITV-Compact model, and dashed lines denote the ITV model [32] predictions.

Propionaldehyde chemistry

Figure 6.6 displays ignition delay time measurements of propionaldehyde/Ar/O_2 mixtures from Pelucchi et al. [51] and Akih-Kumgeh and Bergthorson [1] at three different fuel-air equivalence ratios over a broad range of temperatures. Additionally, predictions with the ITV-Based-Propionaldehyde, the ITV-Compact model, and the model of Pelucchi et al. [51] are shown. The latter functions as a reference model to assess the impact of different base chemistries on propionaldehyde ignition delay times. The ITV-Based-Propionaldehyde model and the model from Pelucchi et al. [51] are in good agreement with the experimental data. Furthermore, only minor discrepancies exist between the ITV-Compact and the ITV-Based-Propionaldehyde model for all validation cases considered in Fig. 6.6.

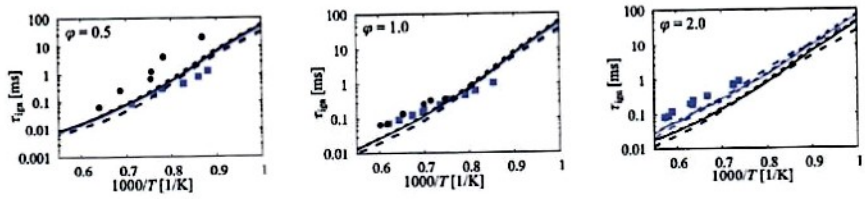

Figure 6.6: Comparison of measured ignition delay times of propionaldehyde/Ar/O_2 mixtures of Pelucchi et al. [51] (blue squares: $p = 1.25\,\text{atm}$; $\varphi = 0.5$, $X_{Ar} = 0.91$; $\varphi = 1.0$, $X_{Ar} = 0.95$; $\varphi = 2.0$, $X_{Ar} = 0.97$) and from Akih-Kumgeh and Bergthorson [1] (black circles: atmospheric pressure; $\varphi = 0.5$, $X_{Ar} = 0.8889$; $\varphi = 1.0$, $X_{Ar} = 0.939$; $\varphi = 2.0$, $X_{Ar} = 0.9298$) to model predictions with the ITV-Compact (solid lines), the ITV-Based-Propionaldehyde (dotted lines), and the Pelucchi et al. model [51] (dashed lines). Experimental data from the work of Akih-Kumgeh and Bergthorson [1] were unavailable for the fuel-rich validation case.

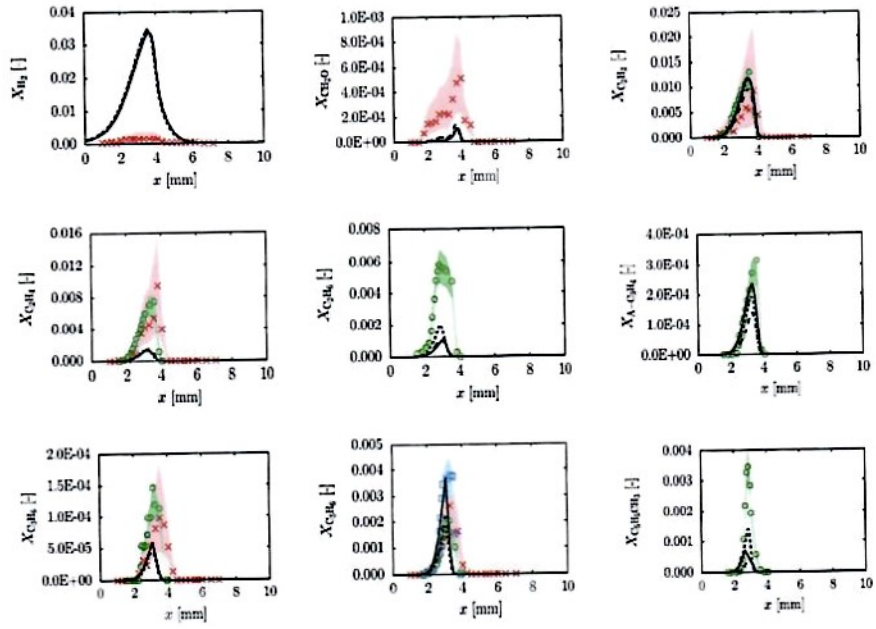

Figure 6.8: Comparison of experimentally measured and predicted mole fractions of small intermediates and hydrocarbons for the CO_2O-Flame, one of the atmospheric anisole diffusion flames investigated by Chen et al. [13]. Experimental data were obtained using three measurement techniques: ToF-MS (red crosses), GC with an Rt-Q-Bond column (blue squares), and GC with a DB-Petro column (green circles). Predictions with the ITV-Compact model, the ITV-Based-Anisole model, and the model of Wagnon et al. [62] are depicted by solid, dotted, and dashed lines. Shaded areas with different colours indicate the measurement uncertainty of the respective techniques. The spatial coordinate x refers to the distance from the fuel nozzle.

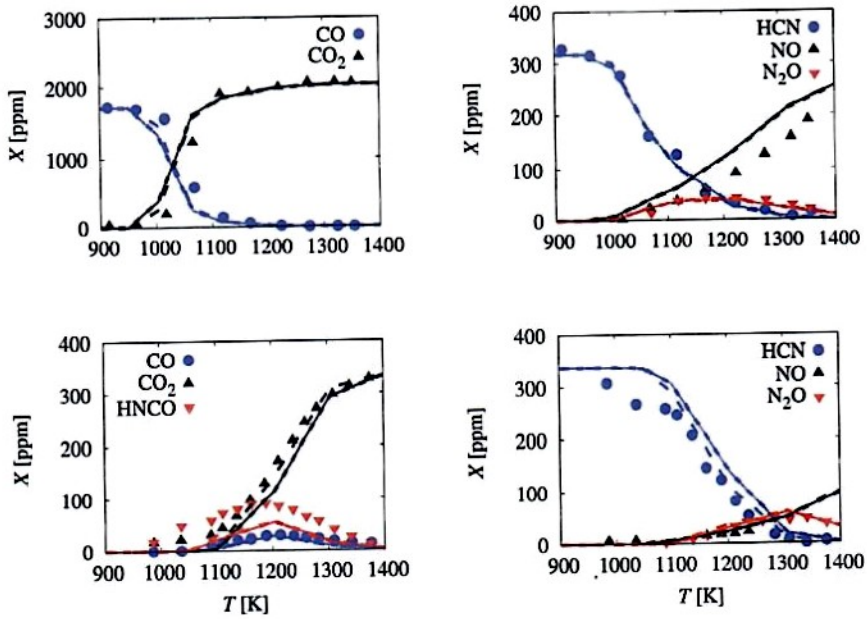

Same here

Figure 6.11: Comparison of flow reactor experimental data (symbols) from Hulgaard and Dam-Johansen [33] and Glarborg and Miller [25] for HCN oxidation at a pressure of 1.05 atm with (upper row, inlet mole fractions were HCN = 318 ppm, CO = 1,710 ppm, O_2 = 2.4 %, and H_2O = 2.8 %, balanced by N_2) and without CO in the inlet (lower row, inlet mole fractions were HCN = 337 ppm, O_2 = 2.6 %, and H_2O = 3.1 %, balanced by N_2) against predictions from the ITV-Compact-NO_x (solid lines), the ITV-Based-NO_x (dotted lines), and the Glarborg et al. [26] (dashed lines) models.

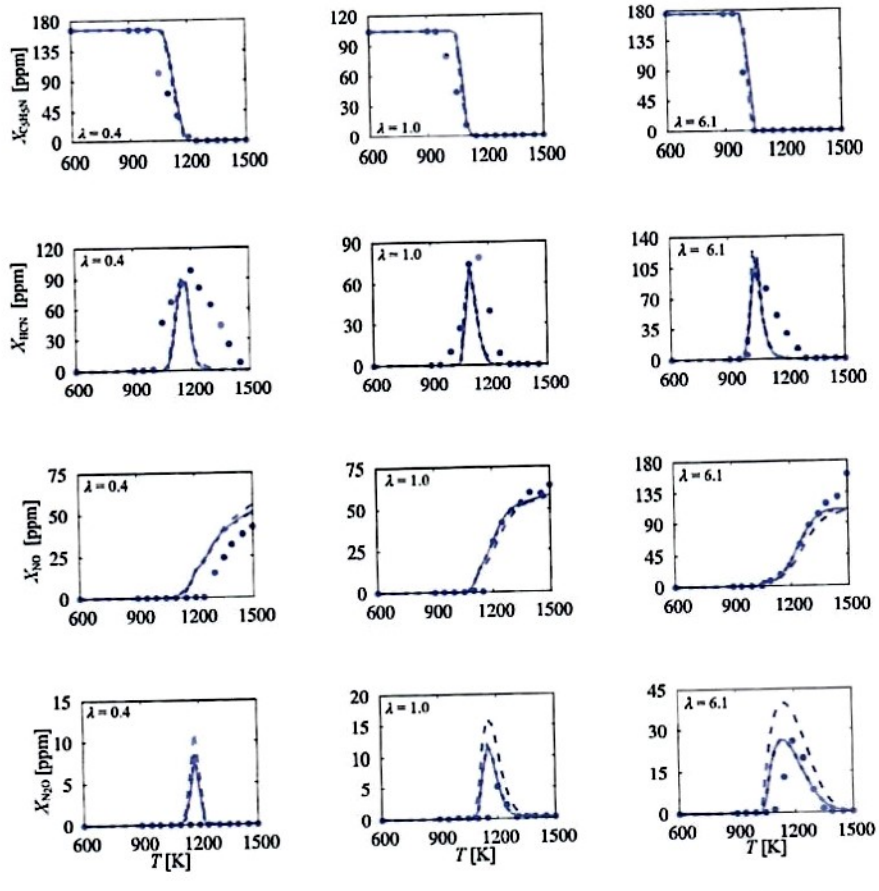

Font size too small

Figure 6.13: Comparison of atmospheric flow reactor measurements (symbols) of Alzueta et al. [2] to predictions with the ITV-Compact-NO_x (solid lines), the ITV-Based-NO_x (dotted lines), and the Shamooni et al. [60] models (dashed lines). Initial conditions correspond to set 3 ($\lambda = 0.4$), set 5 ($\lambda = 1.0$), and set 7 ($\lambda = 6.1$) from Alzueta et al. [2].